Synthesis of Ultrafine Dispersed Coating by Electrodeposition

A THESIS SUBMITTED IN PARTIAL FULFILLMENT OF THE REQUIREMENTS FOR THE DEGREE OF

Master of Technology

In

Metallurgical & Materials Engineering

Submitted

By

Geetanjali Parida

Roll No.208MM105

Department of
Metallurgical & Materials Engineering
National Institute of Technology
Rourkela
2009-2010

Synthesis of Ultrafine Dispersed Coating by Electrodeposition

A THESIS SUBMITTED IN PARTIAL FULFILLMENT OF THE REQUIREMENTS FOR THE DEGREE OF

Master of Technology

In
Metallurgical & Materials Engineering

Submitted

By
Geetanjali Parida
Roll No.208MM105

Under the guidance of

Prof. D. Chaira and Prof. A. Basu

Department of
Metallurgical & Materials Engineering
National Institute of Technology
Rourkela
2009-2010

National Institute of Technology
Rourkela

CERTIFICATE

This is to certify that the thesis entitled, **"Synthesis of ultrafine dispersed coating by electrodeposition",** submitted by **Geetanjali Parida** in partial fulfillment of the requirements for the award of Master of Technology Degree in **Metallurgical and Materials Engineering** at the National Institute of Technology, Rourkela is an authentic work carried out by her under our supervision and guidance.

To the best of our knowledge, the matter embodied in the thesis has not been submitted to any other University/ Institute for the award of any degree or diploma.

Prof. D. Chaira

Dept. of Metallurgical and Materials Engineering

National Institute of Technology

Rourkela- 769008

Date:

Prof. A. Basu

Dept. of Metallurgical and Materials Engineering

National Institute of Technology

Rourkela-769008

Date:

ACKNOWLEDGEMENT

With deep regards and profound respect, I avail this opportunity to express my deep sense of gratitude and indebtedness to Prof. A. Basu and Prof. D. Chaira, Metallurgical and Materials Engineering Department, NIT Rourkela, for introducing the present research topic and for their inspiring guidance, constructive criticism and valuable suggestion throughout in this research work. It would have not been possible for me to bring out this thesis without their help and constant encouragement.

I am sincerely thankful to Dr B. B. Verma, Professor and Head of Metallurgical and Materials Engineering Department for providing me necessary facility for my work. I express my sincere thanks to Prof. B. C. Ray, the M.Tech Project co-ordinator of metallurgy department and also Prof. G. S. Agarwal, Electro metallurgy lab in charge for providing me the necessary facilities for my work.

I also express my sincere gratitude to Prof S. K. Pratihar, for giving me opportunity of using Nano Zetasizer, atomic force microscopy (AFM). I am highly grateful to lab Members of Department of Metallurgical and Materials Engineering, N.I.T., Rourkela, especially Mr. Heymbram, Mr. R. Pattanaik, Mr. U.K. Sahu for their help during the execution of experiments.

Special thanks to my family members ,all department members specially Mr. Tanti, Mr. Samal and all my friends of department of Metallurgical and Materials Engineering for being so supportive and helpful in every possible way.

I am also grateful to the Metallurgical and Materials Engineering Dept. of IIT Kharagpur and National Institute of Foundry and Forge Technology, Ranchi for different characterization facilities.

Date **Geetanjali Parida**

LIST OF FIGURES

LIST OF TABLES

ABSTRACT

Ni-TiO_2 and Ni-ZrO_2 metal matrix composite coatings were prepared by using watt's solution through electrodeposition process. Different weight percentage of Titania and Zirconia powder along with different concentration of surfactant were used for the present study. For the determination of optimum condition of deposition, time of deposition, solution pH, particle amount and surfactant amount were taken as variables, whereas current density and temperature of the bath were maintained constant. To resist agglomeration of ultra fine particles in plating bath due to high surface free energy and to get homogeneous coating, stirring and ultrasonic agitations have been used.

The availability and compositions of coatings were studied by X-ray diffraction spectrum and energy dispersive spectroscopy (EDS). The wear behavior of the pure Ni, Ni-TiO_2 and Ni-ZrO_2 composite coatings were studied by a ball-on-plate wear tester. The microhardness and wear resistance of the coatings increase with increasing of weight percentage of particles content in the coating. The hardness of the resultant coatings was also measured and found to be 375 VHN for Ni coating, 647HV for TiO_2 and 401HV for ZrO_2 depending on the particle volume in the Ni matrix. The results showed that the wear resistance of the composite coatings increased as compared to unreinforced Ni deposited material.

Keywords: Composite coating; Nickel; Titania; Zirconia; microhardness; Wear;

CONTENTS

Title **Page No**

Title **Page No**

Title **Page No**

Chapter 1

Introduction

- Introduction
- Objectives and Scope of the present Study
- Scope of the thesis

CHAPTER 1

INTRODUCTION

1.1 Introduction

Electro co-deposition is one of the challenged processes for improvement of the coated surface. Specially, it is used for the improvement of mechanical properties such as wear and hardness properties of the coating surface. For such case Al_2O_3, TiO_2, ZrO_2,SiO_2, SiC and TiC etc. are the important second phase particle used for the co-deposition and copper, nickel, chromium are used as matrix for the coating. These have the large projected applications for automotive parts, aerospace, printed circuitry and electrical contacts, gold-silver wares and jewelry, musical instruments and trophies, soft metal gaskets, decorative door, light & bathroom fittings [1,2]. The nanosized particles is used by most the researchers for improving, micro hardness, corrosion resistance, nanocrystalline metal deposit.

In economic point of view electrodeposition is an appropriate technique which is used in industries. But as grain / particle size is of major concern, this type of composite coating should ideally be developed at lower temperature range / room temperature by the process of electrodeposition. Again, electrodeposition is simple process for operation and by which uniformly deposited on the heterogeneous surface. The Watt's solution is widely used for Ni deposition; but Watt's bath produces stresses to the plated material which leads to lower fatigue properties. Ultrasonic agitation during deposition is required to lower the stress limit of the plating material along with increased current efficiency and current density of the plating bath which in turn decreases the coating time [3].

The certain important components such as current density, temperature, particle concentration and bath composition are used for smoothening the coating surface and also improve adherent without pitting the surface [4]. Dispersion of the particles in an electrolytic bath is a challenge for the researcher as the ultrafine particles agglomerates into the solution. The parameters are pH, organic surfactant and agitations are maintained for de agglomeration and uniformly dispersion and it also decreases the time period of coating. By referring the above surveys, recent techniques used to produce composite coatings where nanosized particles are suspended in the electrolyte and co-deposited with the metal.

1.2 Objectives and Scope of the Present Study

The present work is aimed to improve surface mechanical properties by electro co-deposition of Ni with dispersed second phase ultrafine titania and zirconia particles individually. The objectives can be listed briefly like below:

1. Electro co-deposition of Ni with ultra fine TiO_2 and ZrO_2 particle such that the mechanical and electro-chemical properties homogeneously throughout the surface
2. Characterizations
    - Microstructure and morphology (SEM, FESEM, AFM)
    - Chemical Analysis and phase identification (EDS, XRD)
    - Surface Mechanical properties (Hardness, Wear)
3. Optimization of the process
4. Correlation with process parameter

1.3 Scope of the thesis

The organization of the rest of the thesis is as follows. The concept of electro co-deposition, their mechanism, applications, parameters for improving deposition, surface morphology changes with parameters and brief review of literatures on nickel co-deposition are provided in chapter 2. A detailed experimental study and different characterization techniques are provided in chapter 3. In chapter 4, characterization of the ultrafine particles along with mechanical properties study of the different co-deposited samples has been presented. A summary of the main findings along with conclusions is presented in chapter 5. Chapter 6 provides references.

Chapter 2

Literature Review

Surface Engineering

Surface Degradation

Techniques of Surface modifications

Electrodeposition

Electrophoretic deposition

Electro co-deposition

Brief Review of Literatures on Nickel co-deposition

Wear

CHAPTER 2

LITERATURE REVIEW

2.1 Surface engineering

Surface Engineering include the total field of research and technical activity used for design, manufacture, investigation and utilization of surface layers for properties better than the core. Surface engineering techniques can be used to develop a wide range of functional properties, including physical, chemical, electrical, electronic, magnetic, mechanical, wear-resistant and corrosion-resistant properties at the required substrate surfaces [1,2]. Surface engineering techniques are being used in the automotive, aerospace, missile, power electronic, biomedical, textile, petroleum, petrochemical, chemical steel, cement, machine tools, and construction industries. Almost all types of materials include metals, ceramics, polymers, and composites can be coated on similar or dissimilar materials [1,2,5].

2.2 Surface degradation

Degradation of material is defined as progressive lose of performance or property with time due to external and internal forces or influences. Surface degradation mainly occurred due to the interaction between surface and environment typically through chemical (oxidation, corrosion) and mechanical interaction (wear, fatigue, fretting etc.) [1,6]. These degradation ultimately entail huge lose or penalty on all engineering system, therefore some important causes of surface degradation should be understood before going into discussion of advanced techniques to improve the surface property. Wear and Corrosion are two important causes for degradation. The scientific study of degradation of engineering materials can be summarized as the rate of decline of performance which is shown in the Figure 2.1.

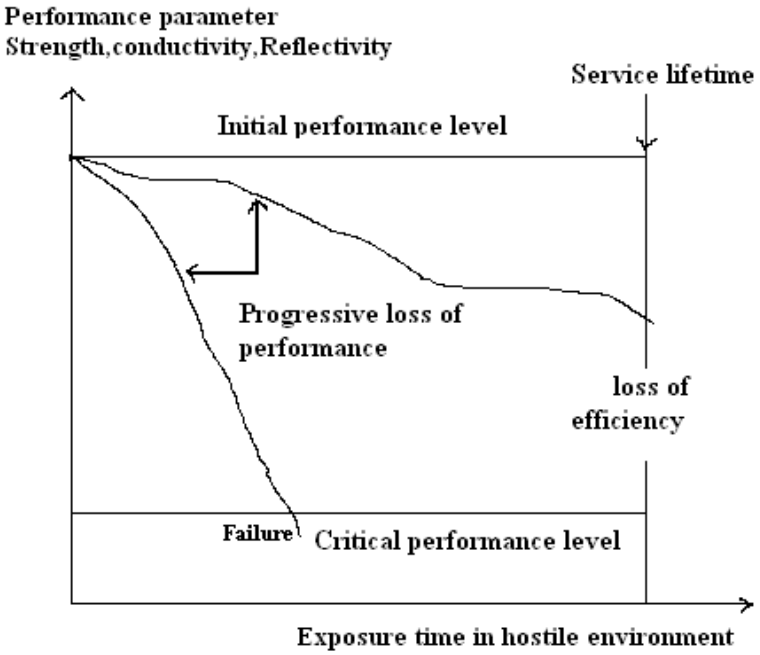

Figure 2.1: Graphical diagram of material degradation as loss of performance of engineering system.

2.3 Techniques of Surface modifications

There are several methods used for surface modifications of materials. The following techniques are few of them used for applying coatings on metals:

- Electroplating–Electroplating is a process of coating, deposition on a cathode part immersed into an electrolyte solution, where the anode is made of the depositing material, which is dissolved into the solution in form of the metal ions, traveling through the solution and depositing on the cathode surface.

- Electroless plating - the process of deposition of metal ions from electrolyte solution onto the substrate, when no electric current is involved and the plating is a result of chemical reactions occurring on the surface of the substrate.

- Conversion coating - the process, in which the coating is formed as a result of chemical or electrochemical reaction on the substrate surface. These are non-metallic coating obtained on metal surface in the form of compounds of the substrate metals.

- Hot dipping - immersing the part into a molten metal, followed by removal of the substrate from the metal bath, which results in formation of the metal coating on the substrate surface.

- Physical Vapor Deposition (PVD) - the process involving vaporization of the coating material in vacuum, transportation of the vapor to the substrate and condensation of the vapor on the substrate surface.

- Chemical Vapor Deposition (CVD) – The process, in which the coating is formed on the hot substrate surface placed in an atmosphere of a mixture of gases, as a result of chemical reaction or decomposition of the gases on the substrate material.

- Thermal spraying – Deposition of the atomized at high temperature metal, delivered to the substrate surface in a high velocity gas stream.

2.4 Electrodeposition

Electrodeposition is a conventional technique, but it is used vastly due to its certain advantages over other as it is of low cost, low energy requirement, capability to handle complex geometry, simple scale-up with easily maintain equipment, good chemical stability, easily maintained equipment and after all very important potential of it is a very large number of pure metals, alloys, composites, ceramics, which can be electrodeposited with grain size less than 100nm [7]. Metals, alloys and polymers can be deposited in this process. Ni, Cu, Cr, Co, Au, Zn etc. are preferred metals in this field [8-11] and Co-Cu, Ni-Co etc. multilayer deposition done in this process [12-14]. Polystyrene, perplex, PTFE, rubbers are the polymer materials apply for coating used in industrial application [2, 15-18]. The coating materials cover the large applications as coatings of engine cylinders, high pressure valves, musical instruments, car accessories, small aircraft microelectronics, aerospace, medical devices, marine, agriculture and nuclear fields.

Nickel deposition is very popular for electrodeposition because nickel coating shows the properties of good mechanical properties, excellent corrosion resistance, high electrical conductivity, good thermal conductivity and good magnetic property [19-21]. Deposition of ceramic particles on metal substrate can be used to improve the mechanical properties of

substrate such as hardness, wear resistance, protection against high temperature, corrosion and oxidation [5, 23-49].

In nickel electroplating method, nickel plate is used as anode and the material which we have plated used as cathode i.e. negatively charged with the DC supply. The Direct current to the anode is oxidizing the metal atoms and allows them to dissolve in the solution. The dissolved nickel ions in the electrolyte solution traveling through the solution and get deposited on the cathode. The rate at which the anode is dissolved is equal to the rate at which the cathode is plated, vis-a-vis the current flowing through the circuit.

The following solutions are used for nickel electroplating [19-21]:

- Watts nickel plating solutions
- Nickel sulfamate solutions
- All-Chloride solutions
- All-Sulfate solutions

Watts solution was developed by Oliver P. Watts in 1916 and it is most popular nickel electroplating solution. Plating operation in Watts solutions is low cost and simple. Bath compositions for watts solution are shown in the table 2.1.

Table 2.1: Composition of watts bath

Electrolytes (Watt's bath)	Nickel sulphate ($NiSO_4.6H_2O$): 350 gm/lit
	Nickel chloride ($NiCl_2.6H_2O$): 45 gm/lit
	Boric acid (H_3BO_4): 37 gm/lit
conditions	pH=3.0-4.5
	Temperature: 55-65^{0}C
	Cathode current density: 5 A/dm^2

Mechanical properties:

Tensile strength: 345-485 MPa

Elongation: 10-30%

Hardness: 130-200 HV

Internal stress: 125-185 MPa

2.4.1 Factors on which adhesion depends

- **Nature of the substrate:** The substrate may be metal, alloying elements of different types of steels and copper alloys. Most commercially available metals are polycrystalline and multiphase system. In general, high density plane (111) shows the least adhesive force [25].
- **Cleanliness of the surface:** Cleaning treatments of the substrate surface prior to the coating operation intended for ensuring strong and uniform adhesion of the coating to the substrate. Mechanical removal of solid particles, burrs, scales and oxides from the part surface by abrasion, blast finishing, vibratory finishing or shot peening [2]. During ultrasonic cleaning**,** scrubbing action produced by numerous small vacuum cavities forming due to high frequency (20 – 45 kHz) sound waves traveling in a fluid, in which the part is submerged [11].
- **Heterogeneity of the surface:** Imperfection and surface defects are the two main cause of heterogeneity [2]. Energy linked with the defect sites are of high in comparison with other sites of the same surface. So there is a variation of heats of absorption or entropy with surface coverage with variation of surface energy. If these heterogeneous samples are prepared for deposition, they are highly worked or deformed as it involved grinding, machining, polishing. The hills and valleys remain on the surface, if observed under high resolution microscope as surface layer become highly strained and rough.
- **Effect of temperature:** The adsorption phenomenon differs from general under the chemisorptions as activation energy concept is associated with this process [2]. Initially adsorption increases with increase in temperature by increase in the quantity of gas absorbed but at maximum temperature adsorption decreases. Chemisorptions on oxide or on metal surface involve considerable activation energies. Clean metal surface have comparable small but significant activation energy.

2.4.2 Surface morphology change with parameters

- **Surface morphology change with current density:** The surface roughness of plated films is changed with current density. Indeed, the surface roughness is high at low current density and becomes small at high current density. Because of the reason a high

density of metal ions and electrons generated at high current densities will be redistributed over the surface according to the magnitude of their repulsive force. This cation redistribution over the substrate surface allows the discharge sites to be more uniformly distributed, making the surface of plated films smoother [52].

- **Surface morphology change with the type of anions:** The surface morphology is affected by the molecular weight and size of anions, which are related to the solution viscosity and the diffusivity of anions toward the anode. A plating solution containing anions of large molecular size, such as sulfate ions, so the Nickel films with a smooth surface can be obtained from a sulfate bath, but the current efficiency is relatively low and the bath tends to produce pitted nickel films. In contrast, the chloride bath has a high current efficiency but produces nickel films with rough surfaces. To improve the current efficiency, while reducing the density of pits and smoothing the surface, both sulfate and chloride salts were mixed into one bath—this is the Watts bath [20,21,52].
- **Surface morphology change with temperature:** High solution temperature generally produces higher surface irregularities. With increasing solution temperature is closely related to the improved supply rate of metal ions, the increased diffusion distance of cations, and the increased surface diffusion distance of adatoms and is can be easily seen that the increased diffusivity allows adatoms to migrate a long distance over the substrate surface which producing large grains [2, 52].
- **Surface morphology change with surface agitation:** Agitation was performed by varying the speed of the magnetic stirring. Nickel films from a non-agitated bath show severe surface irregularities. An increase in stirring speed caused the film surface to become even rougher and secondary surface irregularities were developed on the side face of the primary irregularities, as the solution agitation supplied metal ions to the side face and thus made metal ion discharge possible at such sites [52]. Ultrasonication gives good result in this case. The ultrasonic agitation of the plating bath increased both microhardness and surface smoothness and decreased the residual stresses [5,32].
- **Formation of dendrites:** Dendrites in plated films are often generated under conditions of **low metal concentration/high current densities or of low current dens**ities. An individual dendrite is generally a single crystal, but in some cases, it may be an assembly of fine grains. The films always start as a uniform layer and then a dendrite forms on top of this layer.

This is consistent with the fact that **metal ions present in close contact with the cathode** are initially distributed uniformly over the substrate surface. After the layer formation, a metal-ion denuted zone is created over the surface of different thickness. Dendrites will then nucleate at such regions and their growth will be further accelerated through the tips, if current density becomes very high [52].

2.5 Electrophoretic deposition (EPD)

Electrophoretic deposition is a process in which ceramic particles are suspended in a liquid medium, travel in an electric field and deposit on an electrode. Electrophoretic deposition offers important advantages in the deposition of complex compounds and ceramic laminates [50-52].

2.5.1 Mechanism of electrophoretic deposition

If the charged colloidal particle suspended in an electrolyte solution, there is inhomogeneous distributions of ions, the concentration of counter ions are highest near solid surface and decreases from going outward from the surface. This inhomogeneity leads to the formation of double layer structure, which consists of stern layer and Gouy layer (diffuse double layer) as shown in the figure 2.2. The plane which separated these two layers is called Helmholtz plane. The electrical doubled layer plays essential role in interfacial electrical phenomena on the particle surface and particle-particle interaction in the electrolysis solution [51,53].

The distribution of bath ions is mainly controlled by:

i. **Coulombic force or electrostatic force**
ii. **Entropic force or dispersion**
iii. **Brownian motion**

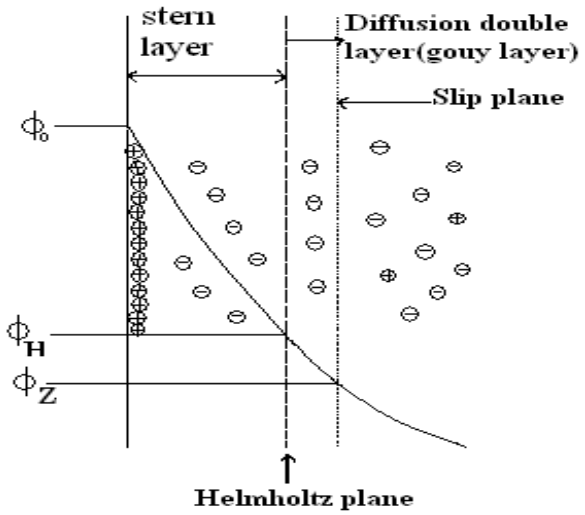

Figure 2.2: Schematic diagram of electrical double layer structure and the electric potential near solid surface with stern and Gouy layers (surface charge is assumed to be positive)

It is impossible to measure surface potential on the colloidal particles. We can measure potential near particle surface by calculating zeta potential.

2.5.2 Measurement of zeta potential of particles

Zeta potential is the potential difference between the dispersion medium and the stationary layer of fluid attached to the dispersed particle. Zeta potential is widely used for quantification of the magnitude of the electrical charge at the double layer. Zeta potential is often the only available path for characterization of double-layer properties. Zeta potential can also be pointed out the degree of repulsion between adjacent similarly charged particles in dispersion. Solution having Small particles control the high zeta potential and it confer stability, i.e. the solution or dispersion will resist aggregation. When the potential is low, attraction exceeds repulsion and the particles get flocculated. So, colloids with high zeta potential (negative or positive) are electrically stabilized while colloids with low zeta potentials tend to coagulate or flocculate [50,51,53].

In general, a zeta potential versus pH curve will be positive at low pH and lower or negative at high pH. There may be a point where the curve passes through zero zeta -

potential. This point is called the isoelectric point and is very important from a practical consideration. It is normally the point where the colloidal system is least stable.

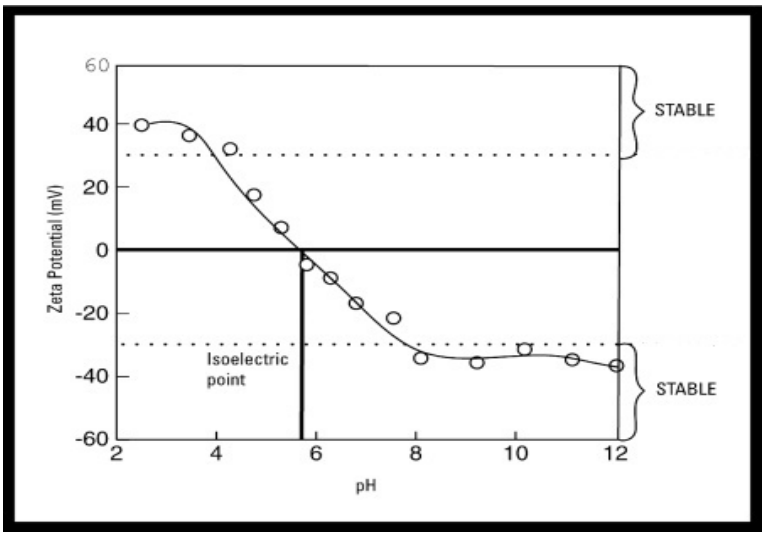

Figure 2.3: pH Vs Zeta potential

In the above schematic Figure: 2.3, it can be seen that if the pH of dispersion is below 4 or above 8 there is sufficient charge to confer stability. However if the pH of the system is between 4 and 8 the dispersion may be unstable. This is most likely to be the case at around pH 6 (the isoelectric point).

2.6 Electro co-deposition

Electro co-deposition of ceramic particle deposition based on electrophoretic deposition (EPD) and electrolytic deposition (ELD). The basic difference between two processes is shown in the following table 2.2. Electrolytic co-deposition is a plating method incorporated of nonmetallic particles into metallic coating. The metals used matrices for electrolytic co-deposition are Nickel, Copper, Chromium, cobalt, iron, gold, zinc, lead alloys etc and the substances used for second phase particles are ceramics or metallic compounds namely.

- Oxides of aluminium, titanium, zirconium, chromium
- Carbides of titanium, tantalium, silicon, tungsten, chromium, zirconium, nickel
- Nitrides of boron and silicon
- Borides of titanium, zirconium, nickel, graphite, stearates, PTFE, diamond
- Sulphides molybdenum and tungsten etc.

In this process the multi-component based metal matrix coatings may be possible by Electrodeposition process. Some metal matrix compounds are Ni-SiC, Ni-Al_2O_3, Ni-TiO_2, Ni-ZrO_2, Cr(N)/TiO_2, Co–Ni–Al_2O_3, Ni–CeO2 etc[5,23-49] .

Table 2.2 : Electrophoretic and Electrolytic Deposition of Ceramic Materials

	Electrophoretic Deposition	Electrolytic Deposition
Medium	Suspension	Solution
Moving Species	Particles	Ions or complexes
Preferred Liquid	Organic solvent	Mixed solvent (water-organic)
Required Conductivity of Liquid	Low	High
Deposition Rate	1-10^3 µm/min	10^{-3}-1 µm/min
Deposit Thickness	1-10^3 µm	10^{-3}-10 µm
Deposit Uniformity	Limited by size of particles	On nm scale
Deposit Stoichiometry	Controlled by stoichiometry of powders used for deposition	Can be controlled by use of precursors

2.6.1 Mechanism of electrolytic co-deposition

As reported above that electroco-deposition mechanism based on two types of mechanism and they are electroplating and electrophoretic deposition mechanisms [50-51]. By using electroplating method, nickel is deposited on the cathode surface where as by electrophoresis method the second phase particle deposited on the cathode surface. This coated surface is also called as metal matrix composite coating. The second phase colloid solution suspended in the electrolytic solution absorbs the positive charge metal ions and gained the positive electric charge (if pH is less than7).

The particles surrounded by the metal ions reach the cathode surface driven by the electrostatic attraction and electrolyte conventions. The particles stick into the cathode surface and discharge. Figure 2.4 shows the schematic diagram of the parallel electroco-deposition process. The retaining capacity of the particles on the cathode surface depends on bonding force between them and also it depends on the interfacial energies of particle-electrolyte, cathode-electrolyte.

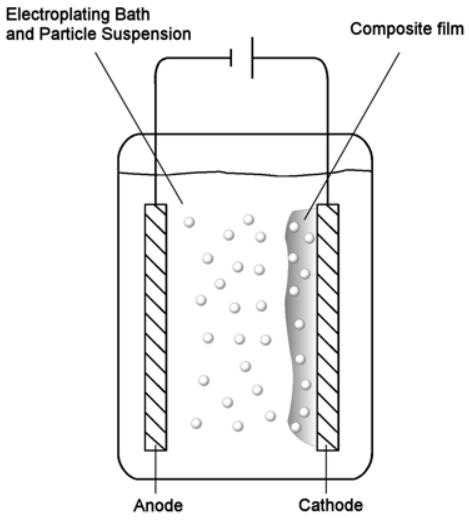

Figure 2.4: Schematic diagram of Parallel plate Electroco-deposition process

2.6.2 Effect of electroplating process parameters on co-deposition

- **Metal ion concentration:** Higher ion concentration leads to denser adsorption of the ions on the particles surface resulting in increase of the driving force of the co-deposition. Increased concentration of the positively charged metal ions enhances the deposition of the particles suspended in the electrolyte.

- **Additives:** Additives promote deposition of the second phase particles from the electrolytic suspensions. Additives promote adsorption of the metal ions on the particle surface and stabilize suspension preventing particles agglomeration.
- **Current density:** Increased current density enhances incorporation of the particles into the deposit.

- **Electrolyte agitation:** Electrolyte agitation increases convection and therefore enhances the flux of the particles reaching the cathode surface, however too intensive agitation may cause adverse effect caused by disconnection and removal of the particles by turbulent streams of the electrolyte.
- **Electrolyte temperature:** Elevated temperature increases the electrolyte flow and the ions mobility due to lower viscosity and density. Higher temperature also causes stronger bonding between the particles and the cathode surface. Thus increased temperature enhances incorporation of the particles into the deposit.

2.6.3 Applications of electro co-deposition

By using this process both metal coating along with non metal powder is coated, so it improves its mechanical (hardness, wear resistance property) as well as electrochemical property (corrosion resistance).

- **Co-deposition of wear resistance particles:** The most popular wear resistant composite coatings are nickel matrix composites with various dispersed phases (Al_2O_3, SiC, WC, diamond, SiO_2, TiO2, and ZrO2) are fabricated by electrolytic co-deposition from nickel sulfamate and Watt's electrolytes. Nickel based wear resistant coatings are used in abrasive tools, measuring tools and gauges.
- **Co-deposition of solid lubricant particles:** Incorporation of solid lubricant particles into a metallic coating improves its antifriction properties. The particles of thermoplastic polytetrafluoroethylene(PTFE), molybdenum disulfide, graphite and boron nitride (BN) are used as the second phase of solid lubricant in the composite antifriction coatings. So the most popular composite antifriction coatings are nickel based with these particles. Copper-graphite and cobalt-BN are other examples of depositions with incorporated particles of solid lubricants [2, 15-18].
- **Co-deposition of corrosion protection coatings:** To enhance the corrosion and oxidation resistance, the strong compounds (oxides, nitrides, carbides, borides) are used as the second phase in corrosion resistant coatings i.e. Al_2O_3, Cr_2O_3, TiO_2, SiO_2, SiC, TiC, Cr_3C_2, Si_3N_4, ZrB. Nickel, cobalt and chromium are commonly used as the matrix materials in corrosion resistant composite coatings.

Examples of corrosion and oxidation resistant composite coatings: Ni-Al_2O_3, Ni-TiO_2, Ni-Cr_2O_3, Ni-TiC, Co-Cr_3C_2, Cr-ZrB [2].

2.7 Brief Review of Literatures on Ni Co-deposition

There are lots of second phase materials which can be used for the co-deposition. Here special importance is given on the powders of ceramics are Titania and Zirconia. The mechanical properties of the TiO_2 and ZrO_2 powder that were selected for the experimental work is given in Table 2.3.

Table 2.3: Properties of TiO_2 and ZrO_2

Property	Value		Units
	ZrO_2	TiO_2	
Density	5.75	4	gm/cc
Hardness	1600 (kg/mm^2) Knoop (100gm)	Microhardness 880HV	
Modulus of Elasticity	207	230	Gpa
Poisson's Ratio	0.32	0.27	-
Compressive Strength	2500	680	MPa

Sun *et al*. [33] prepared the Ni-TiO_2 composite coating on pure copper sheet where titania particles were prepared by sol–gel method. The average grain size of nickel and titania on coating were determined by X-ray diffraction method which was found to be 10 and 12 nm respectively. The phase content of the titania nanoparticles in the composite coatings increased from 6 wt% to 11 wt% with increasing the concentration of the nanoparticles suspended in the electrolytes from100 g/L to 200 g/L. The maximum hardness value and wear rate are 7.5 HV (Gpa) and $43X10^{-15}$ m^3 respectively. The improvement of the friction

and wear properties by the titania nanoparticles attributed to both dispersion strengthening and particle-strengthening effects as studied by Xue et al.[35], Hou et al.[36].

Baghery et al.[38] had done on Ni-TiO_2 nanocomposite coating by DC electrodeposition process. The content of TiO_2 nanoparticles in coating is influenced by current density, stirring rate and TiO_2 nanoparticles concentration in the plating bath. The maximum TiO_2 wt. % in coating is obtained at 30 g/l TiO_2 nanoparticles in the plating bath, current density at 5 A/dm^2 and stirring rate at 180 rpm. The codeposited TiO_2 nanoparticles were uniformly distributed into Ni matrix which shows the improved corrosion resistance and mechanical properties of coating. The hardness and wear performance improved by increasing of TiO_2 wt. % in coating. For 8.3 wt% of TiO_2 the micro hardness was 490HV and wear loss decreases 50% from initial value.

Moller et al. [39] were worked on nanocrystalline Ni/ZrO_2 composite coatings which were produced by co-deposition of ceramic particles during electroplating of Ni in a Watts type electrolyte bath. The amount of codeposited ceramic varied between 0 and 3.7 wt. %. An increase in hardness was observed for the composite material with higher average ceramic content. The maximum hardness achieved was 600 HV at 3.7 vol. % of ZrO_2.

Helena et al. [40] explained that the microhardness of Ni–ZrO_2 dispersion coatings is higher than the microhardness of pure Ni coatings and is directly proportional to the amount of ZrO_2 particles being incorporated in the Ni matrix leading to the structure refinement. Content up to 10 vol. % of ZrO2 was found in Ni matrix. Microhardness (HV0.04) of Ni and Ni–ZrO2 (40 nm, and 200 nm) coatings as a function of pH was also explained by them.

2.8 Wear

Wear is the progressive lose of materials on the working surface of the solid accordingly relative motion between two surfaces. In other words, it is occurred as a result of combination of high stress and constrained motion which initiates surface deformation by contact with the asperities. The adhesions, deformation, frictional heating are the three important conditions by which wears divided into different types [6].

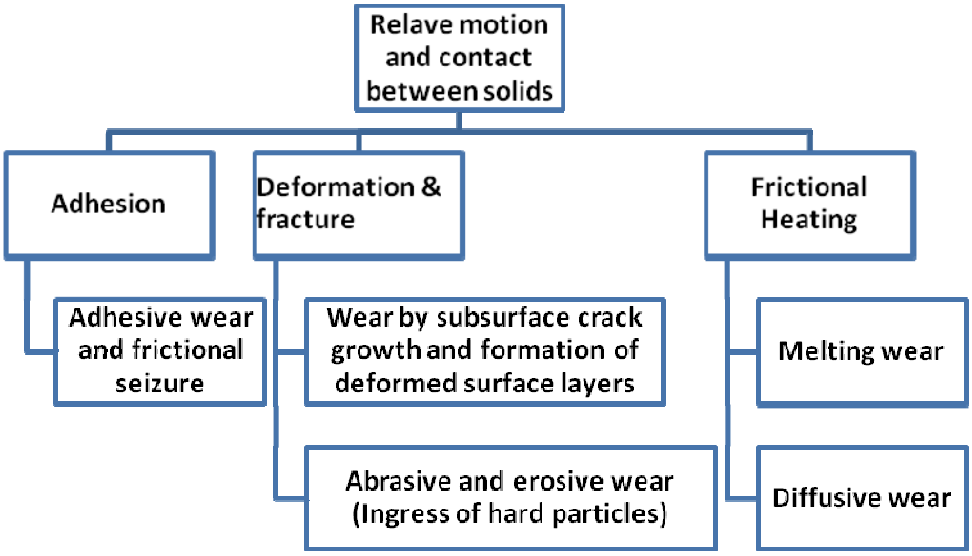

Figure 2.5: The relationship between wear mechanisms and their causes

Figure-2.5 shows adhesion promote adhesive wear and frictional seizer in extreme cases where plastic deformation leads to the formation of subsurface or surface crack growth which leads to the formation of abrasive and erosive wear. If there are high levels of friction and heating occurred then melting wear and diffusion wear has been formed.

2.8.1 The various forms of wear:

Abrasive wear: Rough asperities, hard surface materials or hard particles (non metallic particles) cause abrasion during sliding on the softer material surface. Figure 2.6 shows the schematic of abrasive wear. It damages the interface by plastic deformation or fracture. Rapid abrasive wear occur only when the ratio of particle hardness to material hardness is greater than 1.2. During polishing, the metallic materials are polished by the SiC abrasive paper which is an appropriate example of abrasive wear. Abrasive wear is classified as low stress abrasive (light rubbing), high stress (grinding or crushing) abrasion, gouging abrasion classified by varying stress rate. In gouging abrasion, large particles are removed from surface, leaving dip groves and/or pits. Strain hardening and deformation are the dominant factor in this case.

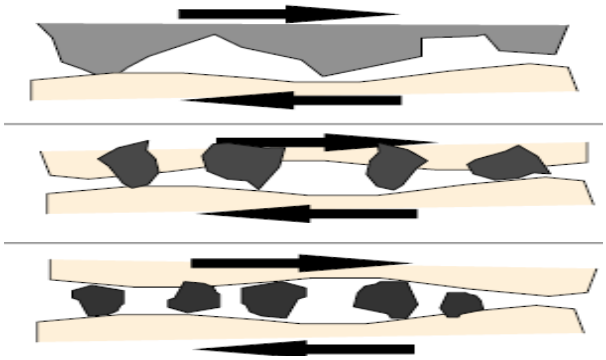

Figure 2.6: The schematic of abrasive wear.

Adhesive wear: Adhesive wear occurs when two contacting metallic components sliding over each other under applied load in the absence of abrasive shown in the figure-2.7. A thin layer of oxide films is supposedly formed. Some are fractured by fatigue process during repeated loading and unloading action resulting in the form of loses particles. The severity of adhesive wear occurs between similar metals in dry sliding. For example sliding between steel test specimens is to cause adhesive wear than between steel and brass or bronze test specimens.

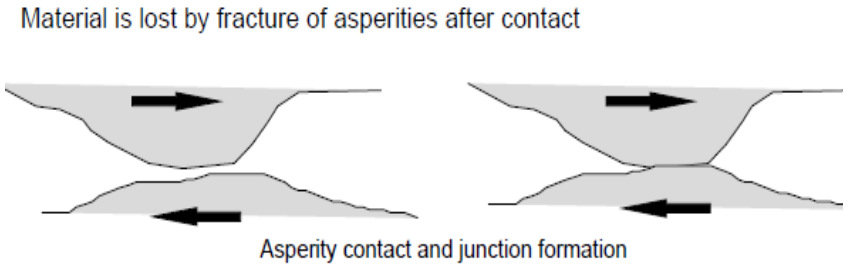

Figure- 2.7: The schematic of adhesive wear.

Corrosive wear: If wear is occurred i.e. removal of materials due to physical interaction of two surfaces in a corrosive media, then the wear rate of the process increases. These types of wear involve disruption and removal of oxide film, Dissolution or re-passivation of exposed metal surface, elastic field interaction at asperities in contact with environment and interaction between plastic deform area and environment. In mining industry abrasive wear is accelerated by wet corrosive environment.

Erosive wear: Erosive wear can be defined as the process of metal removal during the impingement of solid particles on a surface. Erosion can be caused by a gas or a liquid even without the presence of solid abrasive in that medium. When the angle of impingement is small, the wear is equivalent to abrasion. When the angle of impingement is make normal to the surface, then there is plastic deformation or brittle failure. The mechanism of wear isn't constant but it can be controlled by other parameters such as angle of impingement of a particle, its speed, its size and the phase of materials which is shown in the figure-2.8.

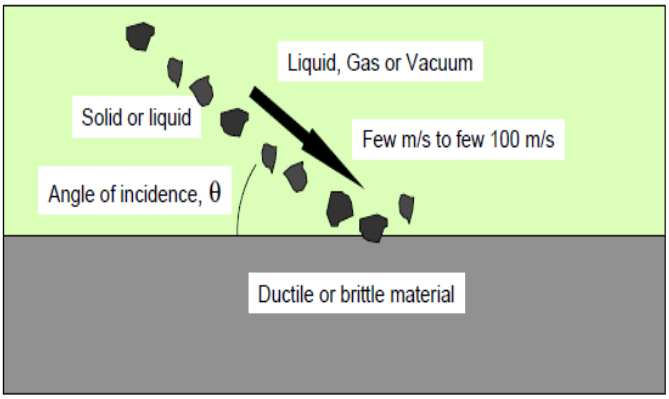

Figure 2.8: The schematic of erosive wear.

The only way to prevent wear is to separate solid surface by a thin film of lubricant or coating materials i.e.1µm thick. Another way is to separate the sliding surface by magnetic levitation in specialized application as it involve expensive superconducting magnets.

Chapter 3

Experimental

Sample preparation

Particle size analysis

Plating Solution Preparation

X-Ray Diffraction Studies

Microstructural analysis

Surface Mechanical Property Study

CHAPTER-3

EXPERIMENTAL

3.1 Sample preparation

Small specimens with approximate dimensions of 10 mm x 15 mm x 6 mm were cut from hot rolled SAE 1020 grade mild steel bar with nominal composition of % C: 0.18-0.22; % Si: 0.1-0.35; % Mn: 0.6-0.7; % Al: 0.01(max); %S: 0.02(max); % P: 0.03; and balance Fe (in wt.%). This steel was selected for the present study as model plain carbon steel used for structural applications.

Samples were prepared by grinding and polishing by using 250, 400, 600 and 800 grit polishing papers followed by cloth polishing. Final polishing was done by 0.25 μm diamond paste. For attaching the samples in the electroplating system holes were made on the samples (to connect wires).

3.2 Particle size analysis

The particle size of ultra fine TiO_2 and ZrO_2 powder which was procured from Inframat Advanced Materials, Formington, USA was checked by Malvern Zetasizer nano series Nano-ZS model instrument. Before measuring particle size, the particle was dispersed in the aqueous bath by 30 minute magnetic stirring followed by 10 minutes ultrasonication. Figure 3.1 shows the photograph of Malvern Zetasizer which can measure particle size from nanometer size to micron size, and zeta potential of suspended particle in a solution. To verify the data available in literature, variation of zeta potential against pH was estimated by the same instrument so that stable suspension pH can be obtained and pH for required cathodic deposition of the ceramic particle can be estimated.

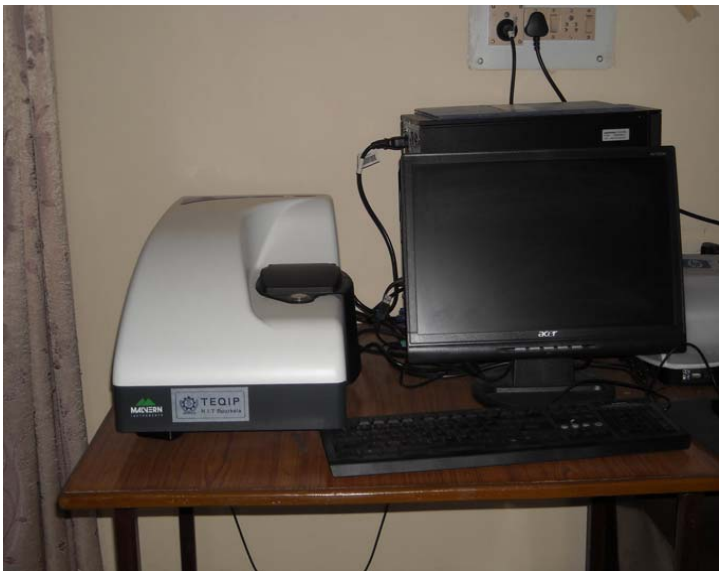

Figure 3.1: Nano zeta sizer (Model: Nano ZS, Malvern instrument).

3.3 Plating Solution Preparation

For electro co-deposition of Ni-TiO_2/ZrO_2, Watt's solution was used as the basic plating bath of Ni. Ultrasonic agitation was used for the dispersion of particle for 1 h just before initiation of the plating process and magnetic stirring was performed during plating. The temperature was maintained by the use of a hot plate and the electro-deposition was controlled by a DC source (APLAB 7103). A stainless steel plate was used as anode where as the prepared specimens were used as cathode. The pH of the plating solution was maintained by adding NH_4OH (for increasing pH) and CH_3COOH (for decreasing the pH). As the isoelectric point (IEP) of TiO_2 is about pH 5.7 and ZrO_2 is 7 [17], the pH was maintained below this value in acidic bath to get co-deposition on the cathode. Moreover, as, at pH ~ 4 the Nickel deposition gives optimal mechanical properties [18] the pH was tried to be maintained at a value of ~ 4. Wetting agent was used to get better adherence as mentioned in the Table 3.1. Surfactant was also used for better suspension of ceramic particles in the bath by changing the contact angle. Thus, different surfactant concentrations (as mentioned in the Table l) were used to improve the coating property.

Table 3.1: The bath composition and deposition conditions

Electrolyte (Watt's bath)	Nickel sulphate ($NiSO_4.6H_2O$): 350 gm/lit	
	Nickel chloride ($NiCl_2.6H_2O$): 45 gm/lit	
	Boric acid (H_3BO_4): 37 gm/lit	
Wetting agent	Sodium dodecyl sulphate: 0.2 gm/lit	
Surfactant	Hexa decylpyridinium bromide: 0, 0.1, 0.3 gm/lit	
pH	~ 4	
Temperature (^oC)	55-65	
Current density	5 A/dm^2	
Plating time	30 minutes	
Dispersion	Titania (TiO_2): 5, 10, 15 gm/lit	Zriconia (ZrO_2): 5,10,15 gm/lit

3.4 X-Ray Diffraction Studies

After deposition, the coating obtained was examined by X-ray diffraction (XRD) to judge the phases formed. Similar study was also carried out on the substrate (before coating) and on the as received ceramic powders. XRD was carried out in 2θ range of $25\text{-}100^0$ and 2 degrees per minutes scan rate using Cu K_α (α= 0.15406 nm) radiation in a Philips X'pert system.

3.5 Microstructural analysis

3.5.1 Scanning Electron Microscopic Studies

Microscopic studies to examine the morphology, particle size and distribution of particles were done by a JEOL 6480 LV scanning electron microscope (SEM) equipped with an energy dispersive X-ray (EDX) detector of Oxford data reference system. The secondary electron imaging was used with suitable accelerating voltages for the best possible resolution. Along with as coated surfaces, cross sectional plane was also observed under SEM. Some samples were observed under a field emission gun assisted scanning electron microscope (FESEM) of model ZEISS: SUPRA 40 for higher resolution micrographs.

Figure 3.2: JEOL JSM-6480LV scanning electron microscopy

3.5.2 AFM analysis

Atomic force Microscopy (AFM) was used for studying the surface morphology and roughness of Ni-TiO_2 and Ni-ZrO_2 coated samples. For this, Veeco id Innova AFM instrument was used for contact mode scan of the samples. For analysis of the AFM data and to get the roughness values, Spmlab analysis software was used.

Figure 3.3: Veeco id Innova AFM instrument

3.6 Surface mechanical property study

3.6.1 Micro hardness measurement

Micro hardness measurements were carried out on the surfaces of TiO_2 and ZrO_2 coated samples. Tests were conducted using a Vickers indenter with 50 g load (Buhler micro hardness tester). Each hardness value reported here is an average of 4-5 measurements on the same sample at equivalent locations. As the coating thickness used here is not wide one, microhardness measurement on the cross section was not carried out.

3.6.2 Wear behavior of coatings

Tribological property including sliding wear resistance of the samples was evaluated using a ball on plate type wear testing instrument having a hardened steel ball (SAE 52100) indenter of 2 mm diameter. DUCOM TR-208-M1 ball on plate wear tester was used for this study to evaluate the wear resistance of the Ni, Ni-TiO_2 and Ni-ZrO_2 coated samples. Sliding distance vs. wear depth were plotted and compared for the different samples. Surface damage caused by wear testing was subsequently analyzed using a scanning electron microscopy to get an idea about the wear mechanism.

Figure 3.4: TR-208-M1 Ball on plate wear tester

Chapter 4

Results and Discussion

Particle size analysis

XRD analysis

Microstructural characterization

Surface Mechanical Properties

CHAPTER-4

RESULT AND DISCUSSION

4.1 Particle size

As raw material characterization, the particle size of the TiO_2 and ZrO_2 procured powder was analyzed by Malvern Zetasizer. Figure 4.1(a) shows the particle size distribution of the TiO_2 powder, consists of two peaks, one below 100 nm (peak value at ~ 30 nm) and the other smaller one above 1 µm. The particle size distribution is bi-modal kind and is wide in nature. But after studying the cumulative value it can be observed that more than 50% particles are sized below 100 nm. Figure 4.1(b) shows the particle size distribution of the ZrO_2 powder and it exhibits only one pack at ~ 940 nm. So unlike TiO_2, ZrO_2 shows larger particle size and single peak of distribution.

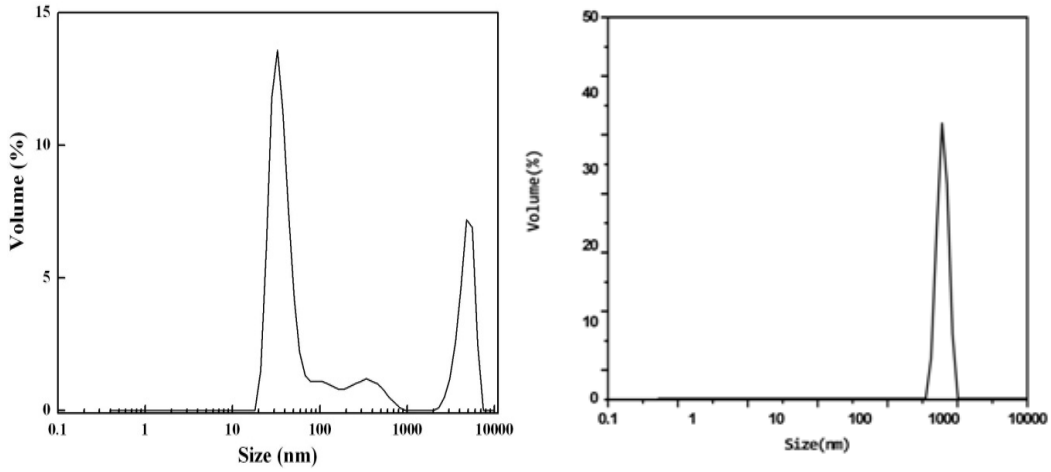

Figure 4.1: Particle size distribution of (a) TiO_2 powder and (b) ZrO2 powder.

4.2 XRD analysis

Figure 4.2 shows the x-ray diffraction (XRD) patterns of procured TiO_2 and ZrO_2 powder. In Fig. 4.2(a) peaks of TiO_2 confirming tetragonal crystal structure could be seen. But, it does not show appreciable broadening though the particles are nanometric in size. The powder source was confirmed to be synthesized by a chemical route which does not introduce strain in the material. So, the broadening observed was only due to the fine crystallite size, not due

to the strain. Thus the XRD peaks do not show huge broadening though the crystallite size is ultrafine. Fig. 4.2(b) shows XRD pattern of as received ZrO_2 powder and it indicates monoclinic crystal structure. Features of this are similar to that of TiO_2 powder.

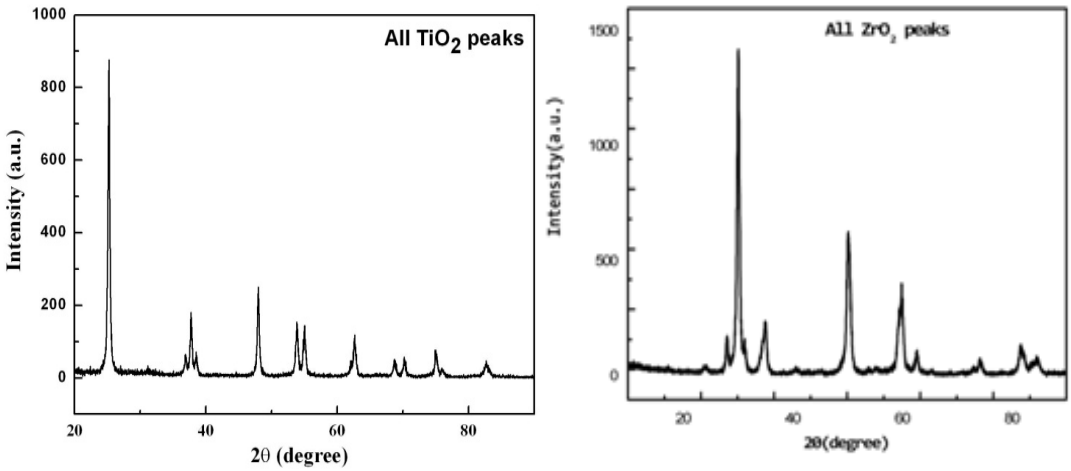

Figure 4.2: XRD pattern of (a) TiO_2 powder and (b) ZrO_2 powder.

XRD study was also carried out on all the coated samples as well as the substrate to identify the phases present on the surfaces. Some of those data are presented here in Figure 4.3 and 4.4. Figure 4.3(a) shows XRD pattern of substrate, nickel coating without addition of ceramic particles and XRD pattern of co-deposited samples (TiO_2 bath composition: 5, 10 and 15 gm/lit.) without addition of surfactant.

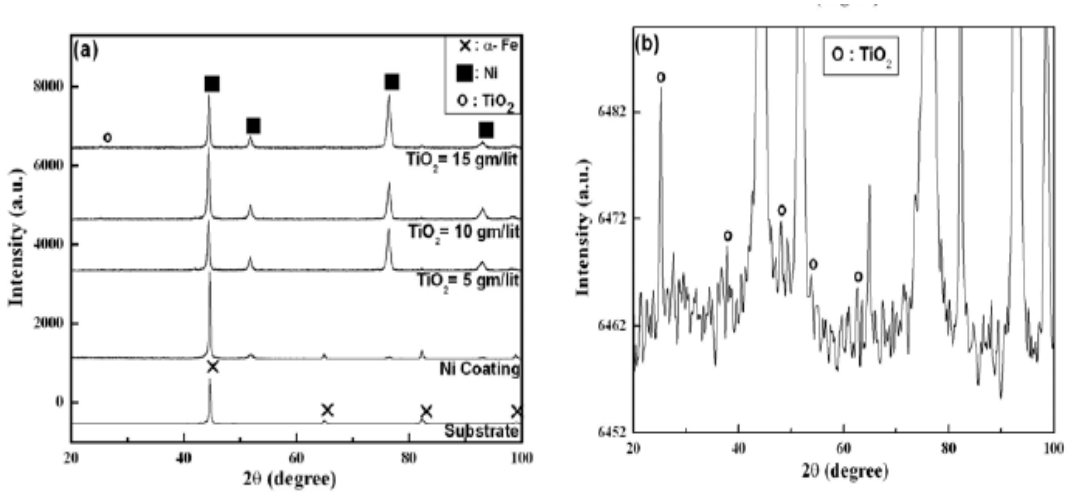

Figure 4.3: XRD pattern of (a) substrate, Nickel coating without ceramic particles, co-deposited samples without addition of surfactant and (b) enlargement of TiO_2 = 15 gm/lit sample data.

The XRD pattern of the Substrate shows only α-Fe peaks, whereas after nickel coating mainly peaks of nickel were observed as predicted. In the three co-deposited samples there was no significant intensity of TiO_2 peaks. To judge it properly one XRD profile (TiO_2 = 15 gm/lit, no surfactant) was enlarged to see the low intensity peaks (Figure 4.3(b)). Figure 4.3(b) shows the various peaks which confirm the presence of TiO_2. With such technique TiO_2 peaks were observed in only 4 samples in the present study. Those are: all the samples with different amount of TiO_2 powder in the bath without surfactant and sample with bath concentration: TiO_2 15 gm/lit and surfactant 0.3 gm/lit. These may happen either due to the absence of TiO_2 in the deposit or due to the presence in very low amount. From Figure 4.3(a) and their enlarged view it can be concluded that during co-deposition trial, TiO_2 deposition was successful with some specific deposition parameters.

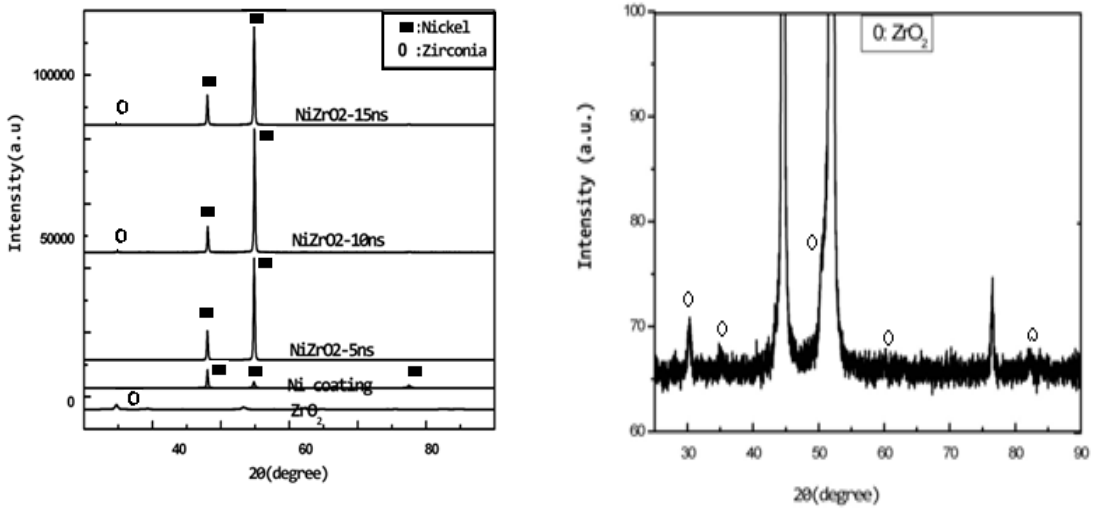

(a) **(b)**

Figure 4.4: XRD pattern of (a) ZrO_2, Nickel coating without ceramic particles, co-deposited samples without addition of surfactant and (b) enlargement of ZrO_2 = 15 gm/lit sample data.

Figure 4.4(a) shows XRD pattern of ZrO_2 powder, nickel coating without addition of ceramic particles and XRD pattern of co-deposited samples having ZrO_2 bath composition: 5, 10 and 15 gm/lit without addition of surfactant. In the three co-deposited samples there was no significant intensity of ZrO_2 peaks. To judge it properly like earlier, one XRD profile of ZrO_2 = 15 gm/lit of no surfactant was enlarged to see the low intensity peaks. Fig. 4.4(b) shows the various peaks which confirm the presence of ZrO_2. Similar data were obtained

from other samples also from which it can be concluded that in these co-deposition trials, ZrO_2 deposition was successful.

4.3 Microstructural analysis

4.3.1 SEM and EDS analysis

Microstructural analysis on the coated surface as well as on the cross section was carried out with scanning electron microscope (SEM). Figure 4.5(a) shows SEM micrographs of sample co-deposited with 10 gm/lit TiO_2 concentration Watt's bath without surfactant. The structure consists of facets of nickel with maximum size below 2 μm along with TiO_2 particles. To judge to particle size, field emission SEM (FESEM) was carried out. Figure 4.5(b) shows that particles are below 100 nm in size. Distribution of the ceramic particles is more or less homogeneous in nature.

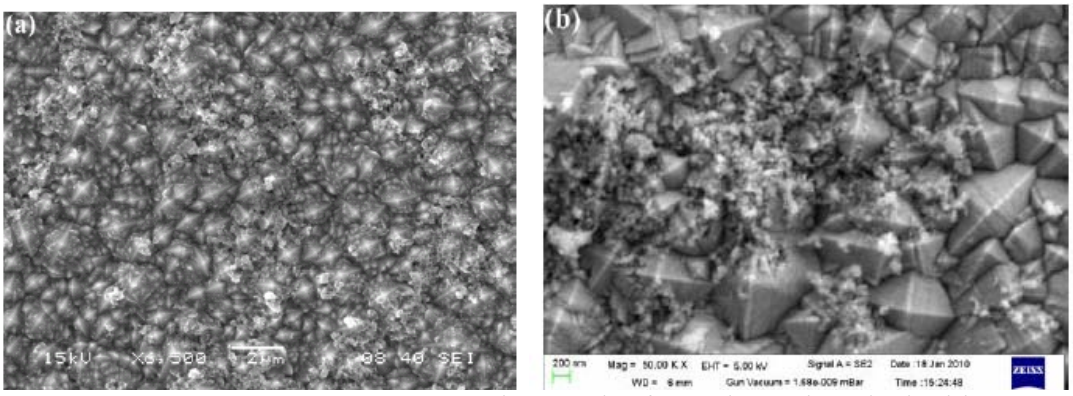

Figure 4.5: (a) SEM & **(b)** FESEM micrograph of sample co-deposited with 10 gm/lit TiO_2 bath Concentration without surfactant.

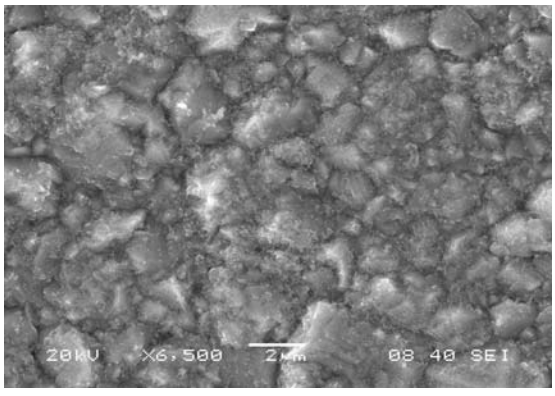

Figure 4.6: SEM micrograph of sample co-deposited with 15 gm/lit ZrO_2 bath concentration without surfactant.

Similar microstructures were also observed when ZrO_2 was used. Figure 4.6 shows SEM micrographs of sample co-deposited with 15 gm/lit ZrO_2 concentration Watt's bath without surfactant. The structure consists of facets of nickel with maximum size more than 2 μm along with ZrO_2 particles.

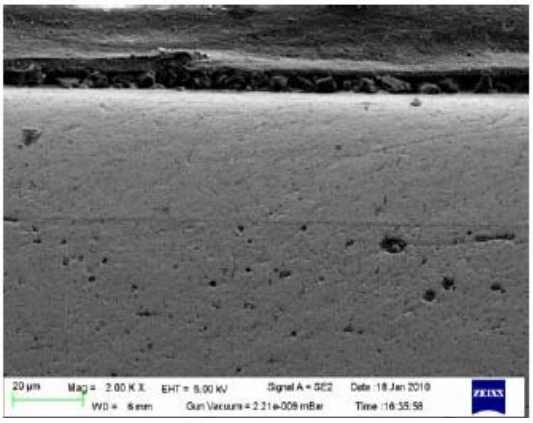

Figure 4.7: SEM micrograph of cross section of sample obtained from 15 gm/lit TiO_2 (without Surfactant) bath.

Figure 4.7 shows the SEM micrograph of cross sectional plane perpendicular to the plane of deposition for the sample obtained from 15 gm/lit TiO_2 and without surfactant. The layer deposited was uniform in nature and the coating thickness observed was about ~ 33μm.

To establish the chemistry of the different phases observed in Figure 4.5 and 4.6, energy dispersive spectroscopy (EDS) study was done on different region on the coated surface. The overall EDS spectrum of the sample which was viewed in Figure 4.4 is shown in Figure 4.8(a). The spectrum confirms the presence of Ti along with Ni and small amount of Fe. Quantitative analysis of the spectra was carried out for all the samples and such data are shown in Figure 4.8(b).

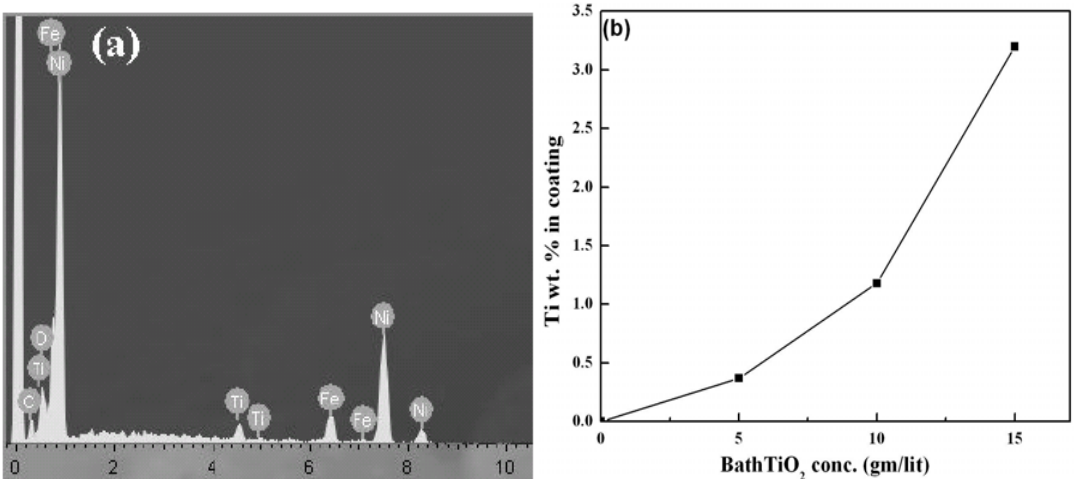

Figure 4.8: (a) EDS data from surface of the sample obtained from 10 gm/lit TiO_2 concentration bath without surfactant. (b) Elemental weight percentage of Ti on the surface of the co-deposited samples (without surfactant).

Figure 4.8(b) shows elemental weight percentage of Ti on the top layer of the coating of the co-deposited samples (TiO_2 bath composition: 5, 10 and 15 gm/lit. without addition of surfactant). Increasing Ti wt. % in the coating is attributed to the increasing amount of embedded TiO_2 particles in the sample. So, from this figure, idea about the variable amount of TiO_2 in the coating can be obtained. In the present set of samples, except these three mentioned in Figure 4.8(b) and sample obtained from 0.3 gm/lit surfactant others show Ti wt. % below 0.1.

Figure 4.9(a) shows different spectrums which confirm the presence of Zr along with Ni mainly. Figure 4.9(b) shows that small increase in ZrO_2 concentration in the bath has improved the embedded Zr weight percentage in the coatings. Zr weight % improves suddenly by changing ZrO_2 bath concentration.

From the observation made from EDS it can be concluded that bath concentration of deposited particles (TiO_2 and ZrO_2) has direct effect on the deposition amount. Surfactant addition only helps with certain values, details of which will be discussed in the next section.

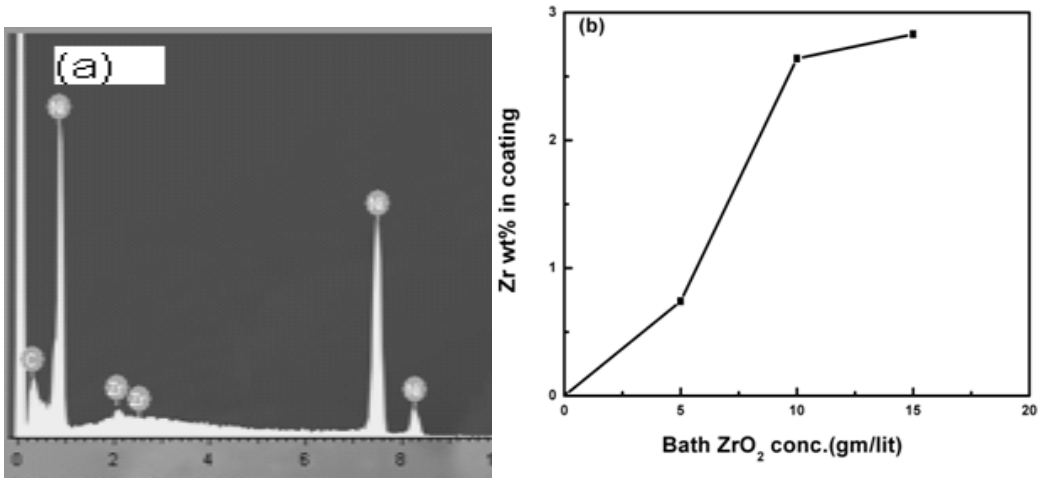

Figure 4.9: (a) EDS data from surface of the sample obtained from 15 gm/lit ZrO_2 concentration bath without surfactant. (b) Elemental weight percentage of Zr on the surface of the co-deposited samples (without surfactant).

4.3.2 AFM analysis

Figure 4.10 shows the atomic force microscopy (AFM) images of different coating surfaces (10 X 10 μm area). Fig. 4.10(a) and (b) shows surface after deposition with 5 gm/lit and 10 gm/lit TiO_2 bath concentration (no surfactant) respectively. The morphology confirms the nature observed under SEM. Moreover there is no such appreciable change in fig. (a) and (b). Fig. 4.10(c) shows surface after deposition with 5 gm/lit ZrO_2 bath concentration (no surfactant). This again shows similar nature.

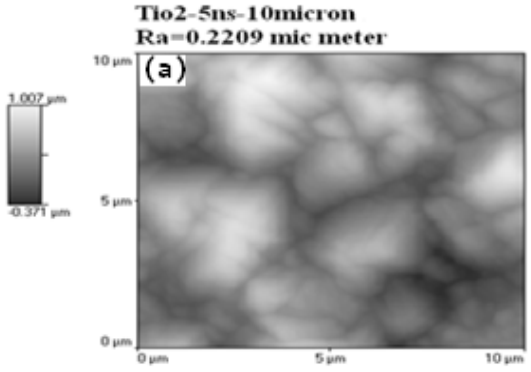

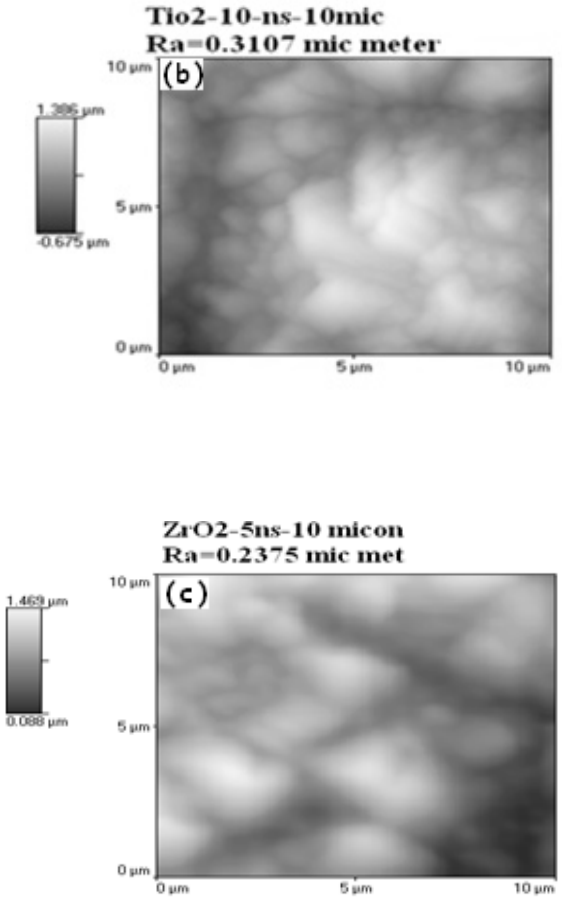

Figure 4.10: AFM image of the coating surface for (a) 5 gm/lit TiO_{2+}, (b) 10 gm/lit TiO_2 and (c) 5 gm/lit ZrO_2 bath concentration without surfactant.

To judge the surface roughness (R_a), AFM data were used and Table 1 shows the mean calculated value of Surface Roughness of these three samples. Samples were scanned with different size of scan area. To get better idea of surface roughness, here for each scan size (5 µm, 10 µm) on a particular sample R_a values are mentioned. From the Table, for TiO_2, it can be observed that with increase in powder concentration in the bath R_a increases. This is due to increase in TiO_2 particle (agglomerated or homogeneous distribution) on the coated surface with increase in bath concentration as mentioned earlier.

Table 4.1: Surface roughness calculation of different samples

Conditions for deposition (No surfactant)	R_a in 5 μm scan area	R_a in 10 μm scan area
Ni-TiO_2 5gm TiO_2 powder	188 nm	314 nm
Ni-TiO_2 10gm TiO_2 powder	220 nm	324 nm
Ni-ZrO_2 5gm ZrO_2 powder	184 nm	250 nm

4.4 Surface Mechanical properties

4.4.1 Microhardness

Figure 4.11 shows variation of microhardness values measured on the coated surface as function of different Particle concentration such as TiO_2 and ZrO_2 and surfactant concentration of the bath for each coating. Hardness values were measured with 50 gm load confirming that the values are not affected by the substrate (coating thickness ~ 33 μm). The base hardness of the steel substrate was measured 184 VHN and that of Nickel coating from Watt's solution was around 375 VHN.

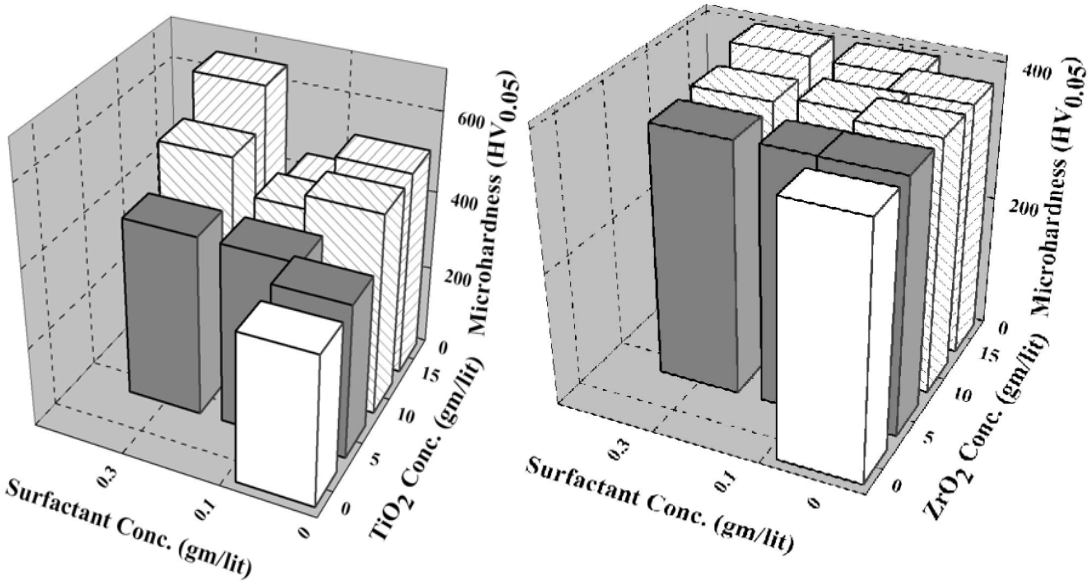

Figure 4.11: Variation of microhardness with (a) TiO_2 and (b) ZrO_2 bath concentration and surfactant concentration.

Microhardness values measured at different points on the surface shows that the microhardness readings are homogeneous. Figure 4.11(a) depicts that with increase in TiO_2 bath concentration the microhardness value increases. For addition of ZrO_2 also (Fig. 4.11(b)) similar trends were observed. From both the figure it is clear that with the addition of ceramic powder in the bath the microhardness values increase even without addition of surfactant in the bath. This can only be attributed to the fact that more amount of ceramic particle got embedded with increase value of bath concentration. Thus dispersion strengthening helps in improving surface mechanical properties. Furthermore, as the particles are ultrafine in nature, the high temperature property of the coating should have gone up due to Zener pinning effect. Maximum hardness value was observed with 15 gm/lit powder and 0.3 gm/lit surfactant bath for both TiO_2 and ZrO_2 powder. The hardness improvement is more prominent in case of titania than zirconia.

It can also be observed from Figure 4.11(a) for TiO_2 powder that microhardness is increased after the addition of 0.3 gm/lit of surfactant in the deposition bath whereas with lower surfactant value there is even decrease also when compared with same TiO_2 bath concentration. Same trend was observed when quantitative EDS analysis was done for Ti. This may be due to the change in zeta potential value after addition of different amount of surfactant. In the present range of study 0.3 gm/lit surfactant shows the best result due to favorable bath condition for deposition of TiO_2. Similar results were presented by Chen *et al.* [47] earlier.

From Figure 4.11(b) for ZrO_2 powder, it is clear that the microhardness value is increased after the addition of surfactant in the deposition bath whereas without surfactant addition there is almost no improvement in hardness even with increase in the powder concentration in the bath. With the addition of 0.3 gm/lit of surfactant in the deposition bath of different ZrO_2 powder, there is no ZrO_2 particle embedded in the coating which is conformed from the EDS analysis. But the hardness still increases and it may be due to the effect of surfactant on the Ni matrix itself. Surfactant thus may have modified the kinetics of Ni nucleation and growth.

4.4.2 Wear study

Figure 4.12 shows the variation of cumulative wear lose (in terms of vertical penetration of the indenter or wear of depth) as a function of sliding distance of different bath composition at an applied load of 5 N at 15 rpm sliding speed on a 2 mm diameter track for 5 minutes duration on the coatings. Fig. 4.12(a) shows such data for TiO_2 co-deposited coating without surfactant. The general trend observed was: wear loss decreases with increase in ceramic TiO_2 powder contents on the bath/coatings whereas Ni coating without co-deposition of TiO_2 shows huge wear loss. So, the trend is similar with microhardness observations. Fig. 4.12(b) shows similar trend for ZrO_2 embedded coatings. It was observed in the last section that microhardness improvement after ZrO_2 addition was not so prominent, but the wear improvement is better. So, dynamic response of surface loading at a sharp point is better in case of ZrO_2 particle. In case of some graphs momentary negative slope could be observed. This may due to welding of soft Ni phase with the hardened steel ball (indenter) resulting in decrease in the wear depth. In general it be concluded that, with increase in ceramic powder contents, the wear resistance of Ni coating increases.

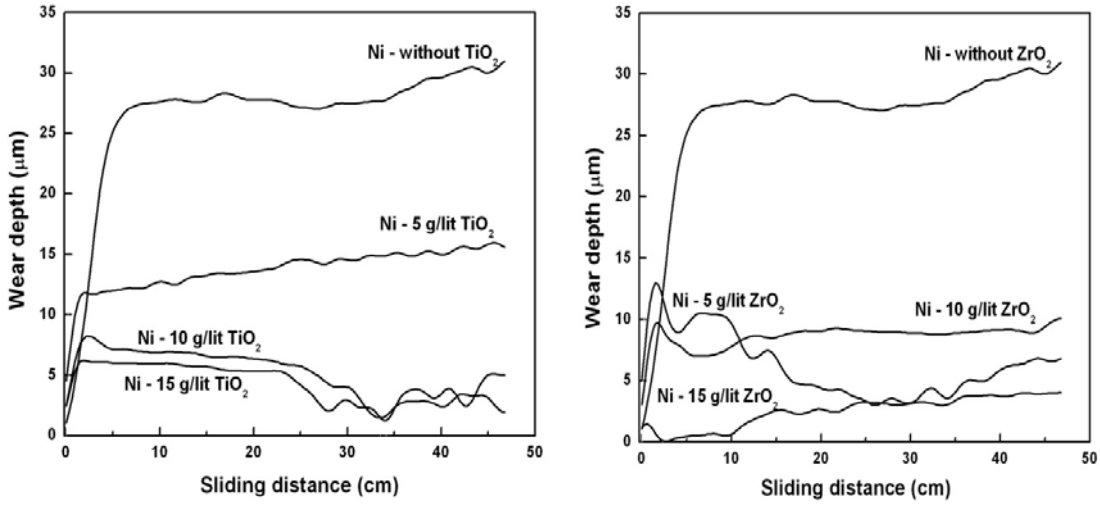

Figure 4.12: Variation of cumulative depth of wear as a function of sliding distance for the coatings: (a) nickel and different TiO_2 bath concentration (5 gm/lit, 10 gm/lit and 15 gm/lit) and (b) nickel and different ZrO_2 bath concentration (5 gm/lit, 10 gm/lit and 15 gm/lit).

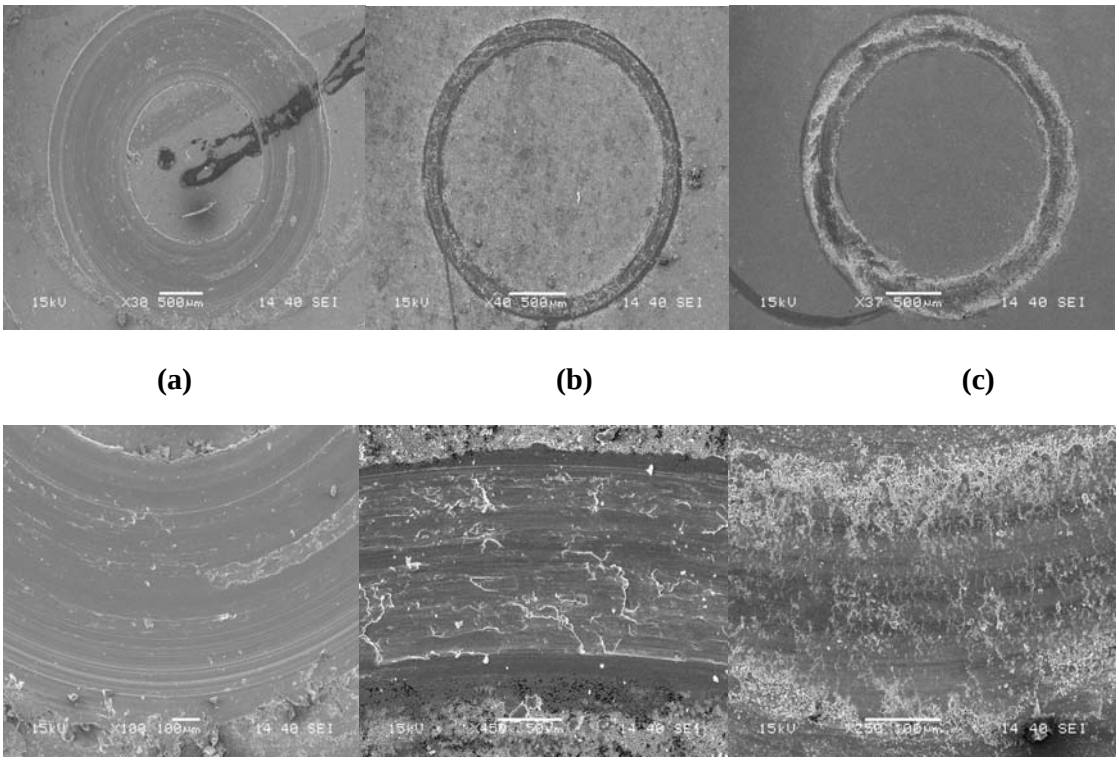

(a) **(b)** **(c)**

(d) **(e)** **(f)**

Figure 4.13: SEM micrograph of wear track of (a) nickel, (b) 15 gm/lit TiO_2 bath concentration coating, (c) 10 gm/lit of ZrO_2 bath concentration coating. Higher magnification micrograph of (a),(b) and (c) in (d),(e) and (f) respectively.

Figure 4.13 shows the scanning electron micrograph wear track on different samples. From Fig. 13(a) and (d) it can be observed that the wear track width of simple Ni coating is far wide and the appearance is smooth due to mostly adhesive wear. In case of co-deposition of nickel and ceramic powder the wear resistance increases in terms of the wear track width (Fig. 4.13(b) and (c)). Same was also observed in Fig. 4.12. When the same tracks were observed under higher magnification (Fig. 4.13(e) and (f)), it was seen that the appearance was not so smooth. There was presence of de-lamination (TiO_2) and abrasive wear (ZrO_2). It can be concluded that after addition of ceramic particle the wear mechanism marginally transforms from adhesive to abrasive nature. This is due to the inherent nature of the ceramic particles and moreover, particles can come out from matrix during wear applications.

Chapter 5

Conclusions

CHAPTER-5

CONCLUSIONS

In this study, an attempt was made to co-deposit Ni-TiO_2 from nano TiO_2 and Ni-ZrO_2 from sub-micron ZrO_2 dispersed Watt's bath. From the detailed investigation, the following conclusions can be drawn:

(i) TiO_2 particles of ~ 30 nm size was successfully co-deposited with nickel on steel substrate where ZrO_2 particles of ~ 1μm size particles was also successfully co-deposited with nickel on the steel substrate but of less amount compared with the titania particles.

(ii) From XRD pattern, the peaks of TiO_2 and ZrO_2 powders are confirmed that tetragonal and monoclinic crystal structure respectively. The peaks of titania doesn't show appreciable broadening though the particles are nanometric in size as the powder is synthesized by a chemical route which does not introduce strain into the material. After co-deposition, the composite coating doesn't show the Titania or Zirconia peaks clearly unless magnified as the weight % of powder are less than 10% for both the Titania and Zirconia cases respectively.

(iii) Nickel is present in the coating with faceted appearance along with TiO_2 and ZrO_2 dispersion respectively where thickness of the coating is about ~ 33 μm after 30 minutes of deposition. From EDS, the weight % of Titanium and Zirconia are known. The dispersed powder of 15 gm/lit and surfactant 0.3 gm/lit in the electrolysis bath are used for the highest weight % reinforcement to be deposited on the composite coatings.

(iv) Though TiO_2 and ZrO_2 particles are not fully de-agglomerated on the deposited layer, the microhardness values are homogeneous and good improvement with respect to the substrate. For Titania, there is maximum 3.5 times and 1.7 times increase in microhardness after addition of dispersion with respect to substrate and pure nickel coating respectively. For Zirconia, there is maximum 2.2 times and 1.07 times increase in microhardness after addition of dispersion with respect to substrate without coating and pure nickel coating respectively. For the both the case, bath condition is 0.3 gm/lit surfactant and 15 gm/lit TiO_2 in watt's

electrolytic bath. Addition of Surfactant is important for Zirconia coating as its particle size was bigger.

(v) The wear resistances of the composite coatings are improved with the increase of weight % of dispersed powder in the electrolysis bath in comparison with the unreinforced Ni coating. There was presence of de-lamination (TiO_2) and abrasive wear (ZrO_2) in codeposited coatings from which it can be concluded that with addition of ceramic particle, the wear mechanism marginally transforms from adhesive to abrasive nature.

Chapter 6

References

CHAPTER 6

REFERENCES

1. Burakowski Tadeusz, Wierzchon Tadeusz, Surface engineering of metals- Principles, Equipment, Technology, CRC Press LLC, 1999.
2. Rastogi M.C, Surface and interfacial science, Narosa publishing house, 2003.
3. Prasad P.B.S.N.V, Vasudevan R, Seshadri S.K and Ahila S, "The effect of ultrasonic vibration on nickel electrodeposition", Materials Letters 17 (1993) 357-359.
4. Przenioslo R, Wagner J, Natter H, Hempelmann R, Wagner W, J Alloy comp, 328, (2001), pp 259.
5. Gul H, Kılıc F, Aslan S, Alp A, Akbulut H, "Characteristics of electro-co-deposited Ni–Al_2O_3 nano-particle reinforced metal matrix composite (MMC) coatings", Wear 267 (2009), pp 976–990.
6. Batchelor Andrew William, Lam Loh Nee & Chandrasekharan Margam, Materials Degradation and its control by Surface Engineering, World Scientific Publishing Co. Pte. Ltd, 1999.
7. Koch C. C, Nano structure materials: Processing, Properties and Potential Applications, Noyes Publications, New York, 2002, 612.
8. Prasad M.J.N.V, Ghosh P, Chokshi A.H, "Synthesis, Thermal stability and Mechanical Behavior of Nano-Nickel", Journal of the Indian Institute of Science 89(2009).
9. Natter H and Hempelmann R, "Nanocrystalline Copper by Pulsed Electrodeposition: The Effects of Organic Additives, Bath Temperature, and pH", J. Phys. Chem, 17 (1996).
10. Vijendra Singh, Physical Metallurgy, Lomus Offset Press, Delhi, 1999.
11. Prasad P.B.S.N.V, Vasudevan R, Seshadri S.K and Ahila S, "The effect of ultrasonic vibration on nickel electrodeposition", Materials Letters 17 (1993) 357-359.
12. Fan chonglun, Piron D. L, "Study of anomalous nickel-cobalt electrodeposition with different electrolytes and current densities", Electrochimica Acta, 41(10) (1996), pp 1713-1719.
13. Uhlemann M, Gebert A, Herrich M, Krause A, Cziraki A, Schultz L, "Electrochemical deposition and modification of Cu/Co-Cu multilayer", Electrochimica Acta, 48 (2003), pp 3005-3011.

14. Fenineche N, Chaze A.M, Coddet C, “Effect of pH and current density on the magnetic properties of electrodeposited Co-N-P alloys”, Surface and Coatings Technology, 88 (1996), pp 264-268.
15. Matthias Seiler, “Hyperbranched polymers: Phase behavior and new applications in the field of chemical engineering”, Fluid Phase Equilibria, 241(1-2) (2006), pp 155-174.
16. Wang Zhen-Gang, Wan Ling-Shu and Xu Zhi-Kang, “Surface engineerings of polyacrylonitrile-based asymmetric membranes towards biomedical applications: An overview”, 304(1-2) (2007), pp 8-23.
17. Haijun Zhao, Lei Liu, Wenbin Hu and Bin Shen, “Friction and wear behavior of Ni–graphite composites prepared by electroforming”, Materials & Design, 28(4) (2007), pp 1374-1378.
18. Ming-Der Ger, Bing Joe Hwang, “Effect of surfactants on Codeposition of PTFE particles with electroless Ni-P coating”, Materials Chemistry and Physics, 76(1) (2002), pp 38-45.
19. Olodnitky D, Gudin N V, Volyanuk G A; journal of electrochemical society, 147(11), 2000, pp 4156-4163.
20. Schario M, "Troubleshooting decorative nickel plating solutions (Part I of III installments): Metal Finishing, 105 (4) (2007), pp 34-36.
21. Schario M, "Troubleshooting decorative nickel plating solutions (Part I of III installments): Any experimentation involving nickel concentration must take into account several variables, namely the temperature, agitation, and the nickel-chloride mix", Metal Finishing, Vol.105 (4), 2007, pp34-36.
22. Vijendra Singh, Physical Metallurgy, Lomus Offset Press, Delhi, 1999.
23. Lekka Maria, Kouloumbi Niki, Gajo Mauro, “Corrosion and wear resistant electrodeposited composite coatings”, Electrochimica Acta 50 (2005), pp 4551–4556.
24. Feng Qiuyuan, Li Tingju, Yue Hongyun, Qi Kai, Bai Fudong, Jin Junze, “Preparation and characterization of nickel nano-Al_2O_3 composite coatings by sediment co-deposition”, Applied Surface Science 254 (8) (2008), pp 2262-2268.
25. Erler F, Jakob C, Romanus H, Spiess L, Wielage B, Lampke T, Steinhauser S, “Interface behaviour in nickel composite coatings with nano-particles of oxidic ceramic”, Electrochimica Acta (2003), 48(20-22), pp 3063-3070.

26. Lampke Th, Leopold A, Dietrich D, Alisch G, Wielage B, “Correlation between structure and corrosion behaviour of nickel dispersion coatings containing ceramic particles of different sizes”, Surface and Coatings Technology, 201 (6) (2006), pp 3510-3517.
27. Hou K. H, Ger M. D, Wang L. M, Ke S T, “The wear behaviour of electro-codeposited Ni–SiC composites”, Wear 253 (9-10) (2002), pp 994-1003.
28. Wu Gang, Li Ning, Zhou Derui, Mitsuo Kurachi, “Electrodeposited Co–Ni–Al_2O_3 composite coatings ”, Surface and Coatings Technology 176 (2) (2004), pp 157-164.
29. Niea X, Leylanda A, Matthewsa A, “Low temperature deposition of Cr(N)/TiO_2 coatings using a duplex process of unbalanced magnetron sputtering and micro-arc oxidation” ,Surface and Coatings Technology, 133-134 (2000), pp 331-337.
30. Szczygieł Bogdan, Kołodziej Małgorzata, “Composite Ni/Al_2O_3 coatings and their corrosion resistance”, Electrochemical Acta,50 (2005), pp 4188–4195.
31. Wang Wei, Hou Feng-Yan, Wang Hui, Guo He-Tong, “Fabrication and characterization of Ni–ZrO2 composite nano-coatings by pulse electrodeposition”, Scripta Materialia 53(5) (2005), pp 613-618.
32. Levashov E. A, Kudryashov A. E, Vakaev P. V, Shtansky D. V, Malochkin O. V, Gammel F, Suchentrunk R and Moore J. J, “The prospects of nano dispersive powders application in surface engineering technologies”, Surface and Coatings Technology, 180-181(1) (2004), pp 347-351.
33. Sun X. J, Li J. G, “Friction and Wear Properties of Electrodeposited Nickel–Titania Nanocomposite Coatings”, Tribol Lett 28 (2007), pp 223–228.
34. Li J, Sun Y, Sun X, Qiao J, “Mechanical and corrosion-resistance performance of electrodeposited titania–nickel nanocomposite coatings”, Surf. Coat. Technol, 192 (2005), pp 331-335.
35. Xue Y, Jia X, Zhou Y, Ma W, Li J, “Tribological performance of Ni–CeO2 composite coatings by electrodeposition”, Surf. Coat. Technol. 200 (2006), pp5677–5681.
36. Hou K.H, Ger M.D, Wang L.M, Ke S.T, “The wear behavior of electro-codeposited Ni–SiC composites”, Wear 253(2002), pp 994–1003.
37. Zhitomirsky I, “Cathodic electrodeposition of ceramic and organoceramic materials. Fundamental aspects”, Advances in Colloid and Interface Science, 97 (2002), pp 279-317.

38. Baghery P, Frazam M, Mousavi A.B, Hoseyni M, “Ni-TiO2 Nanocomposite Coating with High Resistance to Corrosion and Wear”, Surface & Coatings Technology (2010).
39. Moller A, Hahn H, “Synthesis and characterization of nanocrystalline Ni/ZrO_2 composite coatings”, NanoStructured Materials, 12(1999), pp 259-262.
40. Simunkova Helena, Pessenda-Garcia Paola, Wosik Jaroslaw, Angerer Paul, Kronberger Hermann, E. Nauer Gerhard,”The fundamentals of nano- and submicro-scaled ceramic particles incorporation into electrodeposited nickel layers: Zeta potential measurements”, Surface & Coatings Technology, 203 (2009), pp 1806–1814.
41. RameshBabu G.N.K, Jayakrishnan Sobha,”Oxidation characteristics of electrodeposited nickel–zirconia composites at high temperature”, Materials Chemistry and Physics 96 (2006), pp 321–325.
42. Seal S, Viswanathan V, Laha T, Balani K, Agarwal A, “Challenges and advances in nanocomposite processing techniques”, Materials Science and Engineering 54 (2006), pp 121–285.
43. Thiemig Denny, Bund Andreas, “Characterization of electrodeposited Ni–TiO2 nanocomposite coatings”, Surface & Coatings Technology 202 (2008), pp2976–2984.
44. Low C.T.J, Wills R.G.A, Walsh F.C, Electrodeposition of composite coatings containing nanoparticles in a metal deposit, Surface & Coatings Technology, 201 (2006), pp 371–383.
45. Aruna S.T, William Grips V.K, Rajam K.S, Ni-based electrodeposited composite coating exhibiting improved microhardness, corrosion and wear resistance properties, Journal of Alloys and Compounds, 468 (2009) , pp 546–552.
46. Erler F, Jakob C, Romanus H, Spiess H, Wielage B, Lampke T, “Interface behaviour in nickel composite coatings with nano-particles of oxidic ceramic”, Electrochimica Acta, 48 (2003), pp 3063-3070.
47. Chen L, Wang L, Zeng Z, Zhang J, “Effect of surfactant on the electrodeposition and wear resistance of Ni-Al_2O_3 composite coatings”, Materials Science and Engineering, A434, (2006), pp 319–325.
48. Zhou Y, Zhang H, Qian B, “Friction and wear properties of the co-deposited Ni–SiC nanocomposite coating”, Applied Surface Science, (2007).

49. Liping W, Yan G, Qunji X, Huiwen L, Tao X, “Effects of nano-diamond particles on the structure and tribological property of Ni-matrix nanocomposite coatings”, Material Science and Engineering, A390, (2005), 313–318.
50. Furusawa Kunio, Matsumura Hideo, Dekker Encyclopedia of Nanoscience and Nanotechnology, Second Edition, 2009, Colloidal nanoparticles: Electrokinetic characterization, pp-773-785.
51. Boccaccini Aldo R, Zhitomirsky Igor, Application of electrophoretic and electrolytic deposition techniques in ceramics processing, Current Opinion in Solid State and Materials Science, 6 (2002), pp 251–260.
52. Watanabe Tohru, Nano plating-Microstructure control theory of plated film and data base of plated film microstructure, Elsevier Ltd, 2004.
53. Cao, Guozhong, Nanostructures and Nanomaterials – Synthesis, Properties and Applications, Imperical College Press, 2004.